

Thermal Memory Effects on the Linearity of a GaAs PHEMT

C.Accillaro, A.Cidronali, F.Zani, G.Loglio, M.Usai, G.Collodi, M.Camprini, I.Magrini, G.Manes

Dept. Electronics and Telecommunications, University of Florence, Via S. Marta, 3, Florence, 50139 Italy,
acidronali@ing.unifi.it; tel.: +39.055.4796411; fax: +39.055.494569

Abstract – *This paper presents a comprehensive treatment of the nonlinear electro-thermal memory effect arising in a GaAs PHEMT. In particular is demonstrated the way with which the pure nonlinear electrical effect and the electro-thermal one combine and in turn determine a dispersive third-order intermodulation. The analysis is based on an accurate distributed model modified in order to take into account for the dynamic thermal behaviour under large signal operation. The results show a reduction of the intermodulation product in response to a reduction of the two tones frequency spacing, in agreement with the analytical treatment.*

I. INTRODUCTION

The design of microwave transmitters for wireless systems is becoming an increasingly complex task. The main issues related to these applications are the growing bandwidth and envelope variation, imposing stringent requirements in terms of power efficiency and linearity. The actual limitations of such system are due to several aspects of the design; the device technology, the system architecture, the linearization method and finally the accuracy of the analysis tools. In the latter, as a major source of degradation in the performance of RF transmitters, is considered the capability to deal with memory effects. It is widely recognized, [1]-[2] that two class of memory effects exists: electrical and electro-thermal memory effects. In the first class belongs the variation of terminal impedances, due to the biasing and the matching networks, over the input signal bandwidth, its harmonics and baseband frequencies. A careful design of such network would minimize this effects. In the second, the time varying gain caused by temperature-dependent electrical parameters leads to a more serious nonlinear electro-thermal memory effect, the topics of the paper is to provide a comprehensive analysis of this effect for a GaAs PHEMT.

In [5] a distributed model was presented to improve the microwave device models scalability for device with large periphery. In particular, the proposed approach has been based on the identification of a convenient number of intrinsic devices connected to a distributed network. Such a network describes the parasitic access network and how the intrinsic devices, which can be described by means of conventional equivalent circuits or other empirical models, interact each other. A thermal model was added in order to consider the mutual thermal interaction between the intrinsic devices through a network composed of

thermal resistances connected to equivalent voltage-controlled voltage sources (VCVS) generators, which simulate the thermal exchange between all intrinsic devices and current sources that simulate power dissipation of intrinsic devices. The complete model is capable of taking into account both electro-thermal and electromagnetic effects so that great accuracy in scaling properties is obtained also for those large electron devices used in high power applications where self-heating effects cannot be neglected.

In this paper the distributed model is improved to extend its potentiality to the thermal memory effect occurring in a device for power amplification purpose. In particular are investigated the effect of thermal memory on the third order intermodulation product (IMP3), giving a comprehensive discussion of the origin. It is demonstrated that, contrarily with what is observed in other technologies, for the GaAs PHEMT under investigation, the IMP3 reduces as the spacing between tones reduces.

The demonstration of this capability is verified in the paper through the analysis of the third order analysis of a 4x150um GaAs PHEMT manufactured by the OMMIC foundry.

II. THE ELECTRO-THERMAL MODEL

Although the so-called nonlinear low frequency memory effects are generated by thermal dynamic behaviour, by traps in the semiconductor structure and by the bias network, in the following only thermal memory effects are analyzed. The instantaneous dissipated power determines the instantaneous rate of heat that is generated by the transistor. Furthermore, due to the finite mass of the component, thermal impedance includes a capacitive part in addition to the resistive one. Thermal resistance describes just the steady state behaviour, and thermal capacitance is essential for description of the dynamic behaviour. This results in the thermal model reported in Fig. 1.

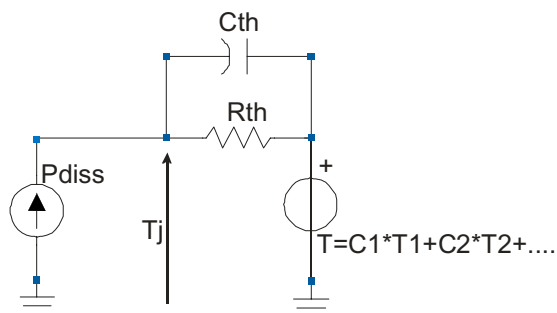


Fig. 1: Thermal model for the intrinsic device

It has been demonstrated [5] that the total thermal distribution is found out by overimposing the individual contributions taking also into account the spacing between elementary thermal sources. Fig. 1 shows the electro-thermal model for the generic intrinsic device with which it is possible to compute the actual finger temperature weighting the temperatures of all others ones. More precisely, once the device structure is completely defined, the contribution of i -th intrinsic device to the j -th is proportional to the temperature of the first and inversely to the mutual distance; this leads to the definition of coupling terms that simply relate the mutual thermal exchange on the basis of their actual temperature and distance. The detailed calculation of the thermal coupling coefficient matrix is given in [5]. The voltage drop across the resistor is hence added to the potential determined by the VCVSs, which multiplies the actual temperature probed from the adjacent intrinsic models, each one including its thermal coupling coefficients. Finally a further VCVS provides the potential associated the bulk temperature. In this way the multi-finger transistor can be seen as a number of elementary intrinsic models, each one including its thermal circuit and whose interaction with the other devices is described by the VCVSs.

From the circuit in Fig. 1 the time varying junction temperature of the elementary intrinsic device is ruled by the relation:

$$\frac{\partial T_j(t)}{\partial t} + \frac{1}{R_{TH} C_{TH}} T_j(t) = \frac{(P_{diss}(t) R_{TH} + T_{AMB})}{R_{TH} C_{TH}} \quad (1)$$

where the local total dissipated power is given by:

$$P_{diss}(t) = V_{DS,dc} \times I_{DS,dc}(t) + P_{RF,in}(t) - P_{RF,out}(t) \quad (2)$$

As it is well known, in GaAs FET the temperature growing produce a drop of drain current and then in transconductance, as the electron mobility decrease with temperature. In order to study the thermal memory effects, a two tones input signal is used, and it is defined in the following expression:

$$v_{in}(t) = V_m (\cos(\omega_0 + \omega_m)t + \cos(\omega_0 - \omega_m)t) \quad (3)$$

by using the above described model it is possible to analyze the fingers temperature, varying the distance between two tones. In the particular case of a 4 finger transistor which a longitudinal symmetry, the thermal behaviour is the one reported in Fig. 2 in the case of $\omega_0=5\text{GHz}$ and an input power level at the two tones of 0 dBm.

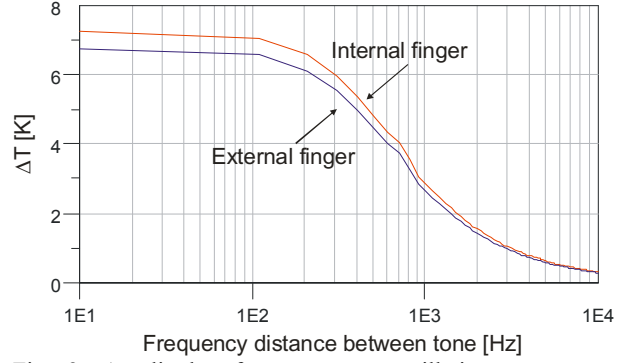


Fig. 2: Amplitude of temperature oscillation respect to frequency distance between tones for two gate fingers, for two tones around 5 GHz and 0dBm power level

III. ANALYSIS OF THE INTERMODULATION PRODUCT DUE TO THERMAL MEMORY

The output signal related to the excitation (3) is modulated by a $2\omega_m$ envelope, this results in a oscillation of the $2\omega_m$ temperature variation; according with Fig. 2, lower is the $2\omega_m$ from the thermal cut off frequency ω_{TH} , higher is the amplitude of the temperature modulation. In the case under investigation, the thermal resistance $R_{TH} = 120 \text{ }^\circ\text{C/W}$ and thermal Capacity $C_{TH} = 3.3 \times 10^{-6} \text{ J/}^\circ\text{C}$, giving a cut off frequency of the thermal circuit $f_{TH} = 400 \text{ Hz}$. The temperature changing produces a bias drain current, $I_{DS,dc}$, change and consequently a transconductance, g_m , variation at frequency $2\omega_m$. This mechanism induces a variation in the total power dissipated in the device. This power variation generates a $2\omega_m$ electrical tone, which in turn generates a IMP3. The latter is then summed to the IMP3 due to the device electrical third degree nonlinearity. In the following, analytical treatment is used to describe the combination among the two distinct IMP3 effects, the nonlinear thermal memory and the conventional electrical one.

Let's consider the power series expansion of the dynamic current flowing through the drain:

$$i_{DS,RF}(t) \cong I_{DS,dc} + g_{m1}v_{in}(t) + g_{m2}v_{in}^2(t) + g_{m3}v_{in}^3(t) + \dots \quad (4)$$

The first order transconductance :

$$g_{m1}(t) = |g_{m1}|(1 + a \cos 2\omega_m t) \quad (5)$$

where the coefficient “ a ” is associated to the amplitude variation with temperature of g_{m1} transconductance.

Considering the baseband variation of $P_{RF,out}$ proportional to $\cos(2\omega_m)$, from (2) is seen that the corresponding variation of P_{diss} is proportional to $-\cos(2\omega_m)$, consequently the same dependency is observed for the temperature. Moreover, from the device physics, a temperature increase determines a reduction of g_{m1} , hence its variation with temperature is like $\cos(2\omega_m)$, finally it is possible to affirm that “ a ” is positive. Considering the above described mechanism as the first contribute to the IMP3, it is possible to introduce:

IV. RESULTS

$$v_{out1}(t) = -g_{m1}R_0(1 + a \cos(2\omega_m t))(\cos(\omega_0 + \omega_m)t + \cos(\omega_0 - \omega_m)t) \quad (6)$$

where the two tones are modulated by the varying transconductance due to the thermal variation.

A same derivation is done for the second order transconductance.

The contribution to the third order transconductance is given by:

$$\begin{aligned} v_{out3}(t) - g_{m3}R_0(v_{in}(t))^3 = & \\ = -g_{m3}R_0V_{in}^3(\cos(\omega_0 + \omega_m)t + \cos(\omega_0 - \omega_m)t)^3 = & \quad (7) \\ = -g_{m3}R_0V_{in}^3[9(\cos(\omega_0 + \omega_m)t + \cos(\omega_0 - \omega_m)t) + & \\ + \frac{3}{2}(\cos(\omega_0 + 3\omega_m)t + \cos(\omega_0 - 3\omega_m)t) + & \\ + 3\cos(3\omega_0t)\cos(\omega_m t) + \cos(3\omega_0t)\cos(3\omega_m t)] & \end{aligned}$$

Combining the above described contribution, the complete expression of the IMP3 products is:

$$\begin{aligned} IMP3(t) = \left[-V_{in}g_{m1}R_0\frac{a}{2} - V_{in}^2g_{m2}R_0\frac{b}{2} - \frac{3}{2}V_{in}^3g_{m3}R_0 \right] \times & \quad (8) \\ \times (\cos(\omega_0 + 3\omega_m)t + \cos(\omega_0 - 3\omega_m)t) & \end{aligned}$$

where “*b*” is the coefficient associated to the amplitude of g_{m2} variation with temperature.

The temperature variations of the g_{m1} , g_{m2} and g_{m3} are reported in Fig. 3. Firstly, is observed that the g_{m2} variation with temperature, can be neglected, so it is possible to suppose that $b \cong 0$. Secondly, the expected temperature variation of g_{m1} is observed.

From these dependencies it is possible to conclude that the IMP3 products generated by nonlinear thermal effects are in opposing to the IMP3 products generated by electrical nonlinear effects.

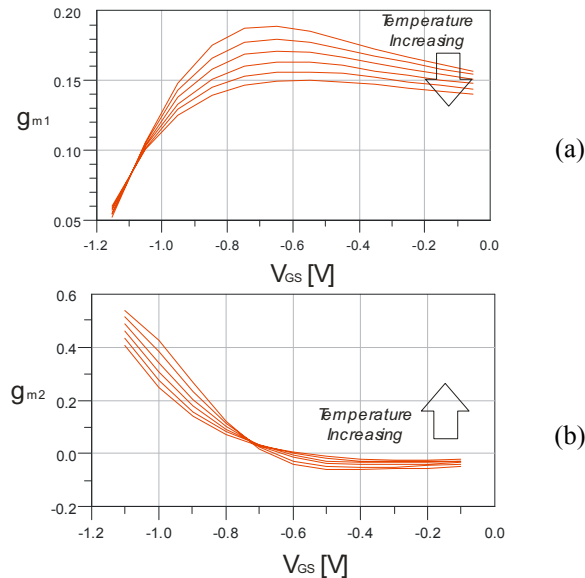
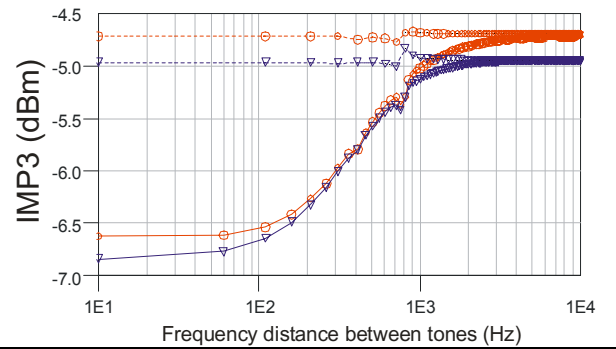


FIG.3: transconductance trend respect to gate source voltage and temperature change, a) g_{m1} , b) g_{m2} .

The validation of the above description is provided by using the distributed model, whose accuracy has been demonstrated elsewhere [5].

In the figure are reported the simulation results, related to the IMP3 generated from nonlinear thermal memory and nonlinear electrical effects, which are compared with the IMP3 generated by nonlinear electrical effects only, as a function of the frequency spacing between the two tone input signal.

As can be seen the level of IMP3 generated by a pure electrical nonlinearity effect, is independent from the two tone frequency spacing. In the case of the presence of thermal memory is observed a reduction of the IMP3 as predicted by (10).



IMP3($\omega_0-3\omega_m$) Electrical ME	IMP3($\omega_0+3\omega_m$) Electrical ME	IMP3($\omega_0-3\omega_m$) Thermal ME	IMP3($\omega_0+3\omega_m$) Thermal ME
—○—	—△—	—○—	—△—

FIG.4: Comparison between IMP3 products by taking into account of thermal effects and without thermal effects, simulated in class A operation.

In conclusion, considering a different transistor technology, e.g. HBT, it is possible to observe a different IMP3 trend, due to the different thermal behaviour with respect to the HEMT behaviour [7]. An increasing of temperature produces an increasing of collector current, hence the dissipated power is increased as well. In Fig.5 is reported the comparison between the two cases. This effect can be compared to the HEMT case, assuming that the corresponding “*a*” factor, in the HBT case assume a value between (-1,0).

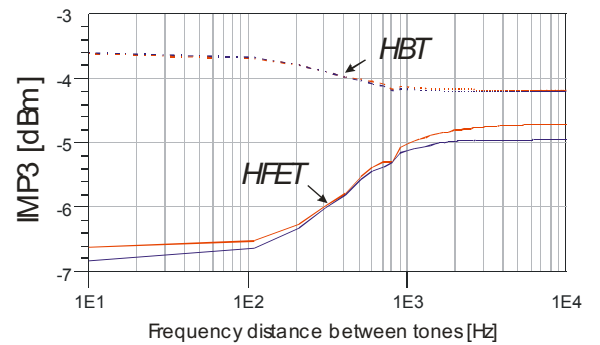


FIG.5: Comparison between IMP3 HBT behaviour and IMP3 HFET behaviour.

V. CONCLUSION

With this paper we have presented a comprehensive treatment of the nonlinear electro-thermal memory

effect arising in a GaAs PHEMT. It has been based on a simplified analytical treatment compared with CAD analysis obtained using an accurate distributed model modified in order to take into account for the dynamic thermal behaviour under large signal operation. In particular is observed a reduction of the third-order intermodulation product in response to a reduction of the two tones frequency spacing. This result, in agreement with the analytical treatment, is due to the particular temperature dependency of the device transconductance. It shows an inverse trend with respect to other technologies, like for example silicon HBT, for which the same analysis confirm the increase of the third-order intermodulation product as the two tones frequency spacing reduces.

ACKNOWLEDGMENT

Research performed in the context of the network TARGET – “Top Amplifier Research Groups in a European Team” and partially supported by the information Society Technologies Programme of the EU under contract IST-1-507893-NOE, www.target-org.net.

REFERENCES

- [1] J. Vuolevi, T. Rahkonen, J. Manninen, “Measurement technique for characterizing memory effects in RF power amplifiers”, *IEEE Trans. on Microwave Theory and Tech.*, vol.49, pp. 1383-1389, Dec. 2003.
- [2] W. Bosch, G. Gatti, “Measurement and simulation of memory effects in predistortion linearizers”, *IEEE Trans. on Microwave Theory and Tech.*, vol. 37, pp. 1885-1890, Dec. 1989.
- [3] N.Le. Gallou, J.M. Nebus, E. Ngoya, H. Buret, “Analysis of low frequency memory and influence on solid state HPA intermodulation characteristic”, *IEEE MTT-S Digest* 2001.
- [4] S. Boumaiza, Fadhel, Ghannouchi, “Thermal memory effects modelling and compensation in RF power amplifiers and Predistorsion linearizers”, *IEEE Trans. on Microwave Theory and Tech.*, vol.51 No.12, Dec. 2003.
- [5] A. Cidronali, G. Collodi, C. Accillaro, C. Toccafondi, G. Vannini, A. Santarelli, G. Manes, “Electrical-Thermal-Elctromagnetic Scalable Model of GaAs P-HEMT”, *European Gallium Arsenide and related III-V Compounds Application Symposium (GAAS) 2003*, pp. 251-254, Munich 6-10 October 2003.
- [6] W. Dai, P. Roublin, M. Frei, “Distributed and Multiple Time-Constant and Its Impact on ACPR in RF Predistortion”, *62nd ARTFG Conference Digest* 2003.
- [7] M. Schroter, “HICUM: A Scalable physics-based transistor model”, *Description of model version 2.1*, Dec. 2000. Available on line ([http:// www.iee.et.tu-dresden.de/iee/eb/comp_mod.html](http://www.iee.et.tu-dresden.de/iee/eb/comp_mod.html)).